JOURNAL OF MATERIALS SCIENCE **40** (2005) 4067–4075

Pore metamorphosis during liquid phase sintering in microgravity

YUBIN HE, SAIYIN YI, JAMES E. SMITH, JR.
Department of Chemical and Materials Engineering, University of Alabama in Huntsville, Huntsville, Alabama 35899
E-mail: jesmith@ebs330.eb.uah.edu

Liquid Phase Sintering (LPS) experiments have been conducted on several sounding rocket flights, Space Shuttle missions and aboard Mir Station, where more than 100 samples were processed for various times. Analysis of those samples revealed considerable pore formation and metamorphosis. Pore filling and coarsening was found in most samples while pore breakup was also found in low liquid volume samples. Pores showed bifurcated behaviors based on their liquid volume fractions. These behaviors resulted from particle rearrangement, particle growth and different diffusion patterns (surface diffusion and volume diffusion) that associated with interfacial energy differences, instabilities, and grain coarsening along the interface between phases. Low liquid volume fraction and the presence of the agglomeration, which results in high local solid volume fraction, enhances the volume diffusion during the process which causes the pore breakup. This paper attempts to show pore bifurcation behavior, which produces either smaller pore by a breakup mechanism or coarsened pore of large size. An initiation mechanism induced by grain growth, capillary force and other weak forces is proposed and the results from theoretical analysis and CFD numerical simulation are presented.

1. Introduction

Liquid Phase Sintering (LPS) is a widely used industrial powder metallurgy process. For some sintered materials such as cutting tools or inserts, high porosity is considered an unwelcome phenomenon. In manufacturing these materials, considerable efforts have been directed towards attaining complete densification and drive the pore volume to zero [1]. Ideally, obtaining the maximum density, termed the theoretical density, would require a pore free composite. On the other hand, for porous materials such as metal foams, hydride catalysts and sustainable high-temperature synthesized (SHS) materials, high porosity is desirable [2]. Achieving high or low relative densities often leads to increased costs and manufacturing complexity. Therefore the pore study is crucial both practically and theoretically.

Pore metamorphosis during liquid phase sintering (LPS) in unit gravity is very "erratic" [3]. In unit gravity processing, density differences cause sedimentation within the sample, which contributes to solid migration, non-uniform coarsening and anisotropy in the mechanical and material properties of the sintered compacts [4–6]. Even for systems like Co-Cu who has small density difference between two phases [7, 8], it is not possible to eliminate buoyancy effects such as pore migration and sample slumping in unit gravity [9]. Processing in microgravity environment provides a unique opportunity to isolate transport from sedimentation mechanisms, thereby permitting the study of transport effects on macrostructure, pore morphology and microstructure.

Pores are not buoyant in microgravity as they are in unit gravity and therefore remain in equilibrium with the solid and liquid phases during LPS. The study of pore metamorphosis in microgravity is unique because the origin, behaviors and lifetime of a pore can be studied. However, in microgravity, removing sedimentation driven convection does not produce a static system. Pore metamorphosis driven by surface tension and capillary forces is still present in microgravity processed samples. Here the terminology of pore is subclassified as a void when low vapor pressure exists and a bubble when inside pressure is high [10]. The surface properties of a pore as well as the shape of the pore are also affected by the size of surrounding particles and the liquid flowing around the pore.

There are three fundamental stages associated with the process of liquid phase sintering namely rearrangement, solution-reprecipitation and solid state diffusion [5]. At the beginning of liquid formation, because of the solubility and capillary force, liquid will quickly flow into particle capillaries, wet the particles, cut off pore network and isolate pores from each other. This process leads to closed-pore structures due to the reduction of total interfacial energy. Pores continue to metamorphose during the later stages of liquid phase

sintering. In the past many powder compact samples from the Fe-Cu, Co-Cu, W-Cu and W-Ni-Cu systems were processed during liquid phase sintering experiments aboard four sounding rockets, five different Space Shuttle missions and twice aboard Mir station [11–14]. Pore deformation was observed in all samples. Detailed studies have shown that three pore deformation behaviors exist among the samples, namely, pore breakup, pore filling and pore coarsening. In this paper some results from Fe-Cu samples and Co-Cu samples will be presented to further discuss the mechanism of pore metamorphosis during microgravity liquid phase sintering. The understanding toward those pore formation and metamorphosis could improve ground-based processing and increase commercial applications of these materials both on ground and in microgravity.

2. Experimental details

LPS of powder compacts were conducted aboard the Consort sounding rocket, three Space Shuttle missions and aboard Mir Station twice. The compositions were selected to yield different volume percent of the liquid copper phase during sintering. The furnace module for these flights was configured to exceed the melting point of the additive materials (Cu in Fe-Cu and Co-Cu systems). The samples were processed for 2.5 min aboard the Consort 4 sounding rocket, 5 min aboard STS-57, 17 min aboard STS-60 and 66 min aboard STS-65, using the Equipment for Liquid Phase Sintering Experiments (ECLiPSE) flight furnace and quench system, described elsewhere [13, 15, 16]. The processing time for Mir samples ranged from 10 min to 330 min with Russian Optizon furnace.

The powders were supplied and graded by Alfa (Catalog #00622 for Cu, #10455 for Co) and were used as received without further modification. Samples with different Cu volume fraction (50, 60, 70 and 80%) were prepared. No was or particle lubricants were used in order to minimize contamination of the compact. They were weighed in air and blended in a rotary mixer, the speed of which was optimized using the relationship RPM $= 32/(\text{cylinder diameter})^{1/2}$ [17]. The homogenized powders in the mixer were then transferred into a zinc stearate lubricated die in which the green compact was formed under approximately 110 Mpa pressure for one hour [12, 15, 16, 18, 21]. A carver laboratory press was used in this process in order to obtain a green compact (unsintered compact) with 70% theoretical density. The gauge pressure was elevated to two tons per square inch (tsig) for three min followed by seven tsig for one hour. The modicum pressure of 110 Mpa was selected by trial-and-error to minimize forced shape accommodation, compact swelling and solid skeletal formation within the compact, while developing enough structural integrity to tolerate launch loads [12, 15, 16, 18, 21].

The pressed compacts were reduced in a tubular reactor under a flowing gas mixture of 5% H_2 with the balance He, following a time and temperature profile designed to remove contaminating oxides and lubricants. The peak temperature is 300°C. The samples were then separated by stainless steel or ceramic shims. Finally they were put into ampoules that held samples in furnace and sealed in He gas chamber. The samples was processed in vacuum aboard several Space Shuttle missions and in Mir Station.

The processed Co-Cu samples were analyzed using metallurgic microscope and Scanning Electron Microscope (SEM). The pore size was measured using IMAGEN Video Marking and Measurement System, SigmaScan Image Measurement System and Buehler's Omnimet Advantage Image Analysis System.

3. Pore formation and metamorphosis in Cu-Fe and Co-Cu samples processed under microgravity

3.1. Pore breakup in Fe-Cu samples

Examination of the samples taken from 30%Cu-Fe sintered aboard the Consort 4 sounding rocket and in ECLiPSE-HAB2 aboard Space Shuttle (STS-57, 60 and 63) showed that pores within the microstructure underwent metamorphosis, where larger pores broke up into strings of smaller spherical pores as the processing time increased [11, 19–21]. Fig. 1 is a SEM micrograph of 30vol.%Cu sample showing that both individual pores and networked pores. The individual pores transformed from the initial networked pores prior to melt after 2.5 min of processing. Fig. 2 showed that the grains had coarsened considerably for 30vol.%Cu sample after 5

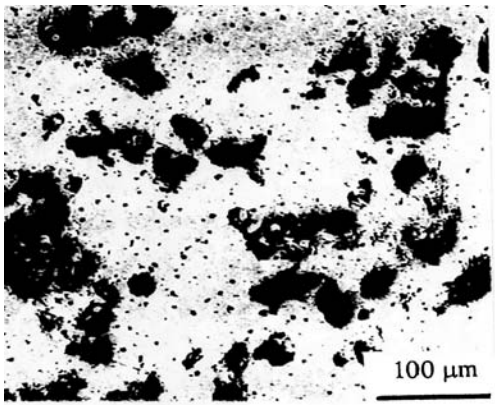

Figure 1 SEM-BEI microphotograph of Fe-33Cu sample processed 2.5 min.

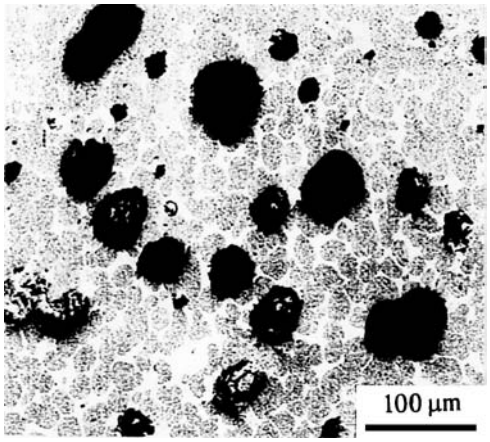

Figure 2 SEM-BEI microphotograph of Fe-33Cu sample processed 5 min.

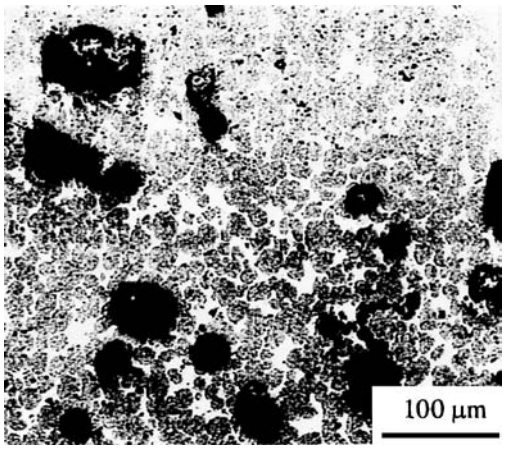

Figure 3 SEM-BEI microphotograph of Fe-33Cu sample processed 17 min.

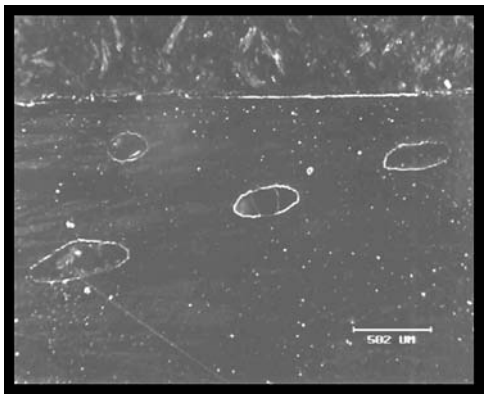

Figure 4 A string of pores (30%Cu-Fe, processing time 330 min).

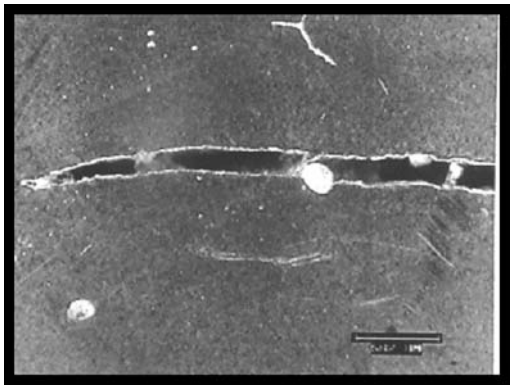

Figure 5 A pore is undergoing breakup (20%Cu-Fe, processing time 330 min).

min processing, most networked pores had closed, and the pores were more spheroidized. More significantly, several of these individual spherical pores were linearly arranged. This suggests that they were originally part of ellipsoidal pores that were broken up by ovulation. Dumbbell shapes were observed as a result of necking, suggesting that these pores were in the process of breaking up. Micrograph of 30vol.%Cu sample that was processed for 17 min (Fig. 3) showed additional pores arranged in linear strings, some of which were dumbbell shaped. The pore shapes were more spherical and much smaller in size. This strongly indicates that pores were breaking up and the increased processing time resulted in pore of smaller sizes and regular shapes. Micrograph of sample processed for 66 min showed that the pore sizes and population did not change much as the processing time was increasing from 17 min to 66 min. At the mean time, Pore coarsening is also observed in samples after long time sintering. For high volume fraction samples, pore coarsening and pore filling was found instead of pore breakup.

To further study the pore metamorphosis with respect to sintering time and solid volume fraction, some Fe-Cu samples and Co-Cu samples were processed in Mir Station along with some Ag based compacts. Processing time up to 330 min and the highest solid volume fraction is 80%. Analysis of those samples showed that pores exist even when sample was processed in vacuum [22].

The microstructures of Fe-Cu samples exhibited both pore breakup and coarsening during sintering process, based on liquid volume fraction. For low liquid volume-fraction samples, pore breakup dominants. Fig. 4 shows a string of pores, which was broken from one pore in 70vol%Fe-Cu sample. Fig. 5 shows a pore undergoing breakup in 80vol%Fe-Cu sample. It can be seen that the liquid copper is formed inside the pore to form a bridge and broke the pore into several pieces. When this pore is fully isolated by the liquid copper, the pressure changes due to the surface tension will cause each small pore to shrink. As a result of pore breakup, the densification will be higher.

As the liquid volume increase, the pore-size increases and the total number of pore decrease. For 50%Cu-Fe sample, only a couple of pores left with one pore close to 2 mm in diameter. Figs 6 and 7 shows a typical pore in 40%Cu-Fe and 50%Cu-Fe samples, respectively. The densification will also be small since pore volume increases. Fig. 8 shows the densification of 20%Cu to 50%Cu samples after 330 min sintering. The densification data clearly shows that highest liquid volume fraction samples has lowest densification. This is the same as densification changes in Fe-Cu samples processed in sounding rockets and Space Shuttle missions where 30% samples showed pore breakup and high densification, while 40% and 50% samples did not [20].

The pore Fe-Cu samples showed bifurcated behavior. Liquid volume fraction seems to be a key parameter

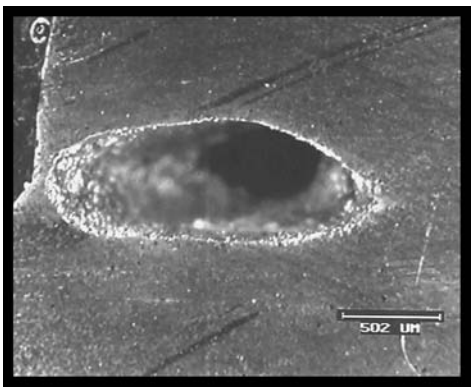

Figure 6 Pore in 40%Cu-Fe sample, processing time 330 min.

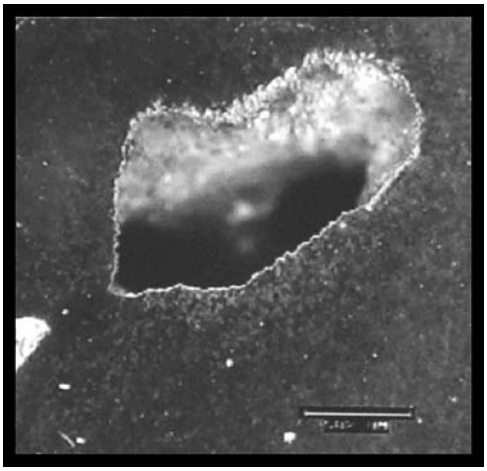

Figure 7 A cylindrical pore in 50%Cu-Fe sample, processing time 330 min.

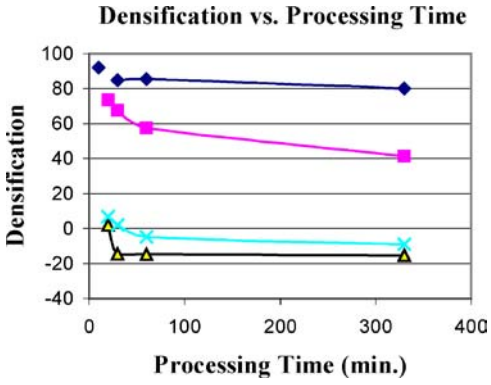

Figure 8 Densification of Fe-Cu processed in mir station for 330 min sintering.

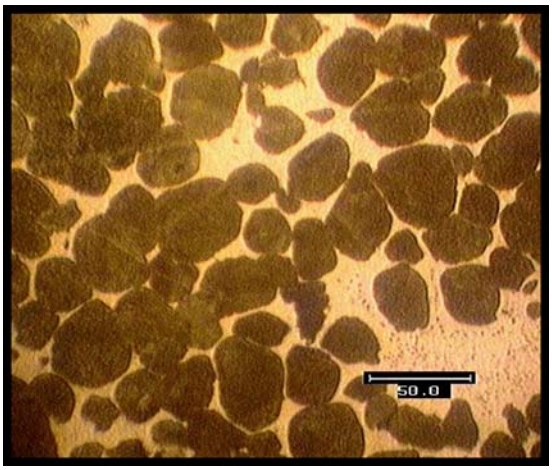

Figure 9 microphotograph of 70%Co-Cu sample processed for 2.5 min.

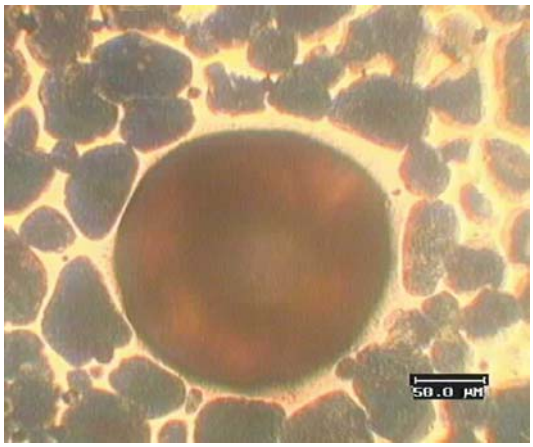

Figure 10 Pore filling in a Co-Cu sample.

in pore changes. Samples with liquid volume fraction higher than 30% showed pore coarsening dominant whereas the pore breakup dominants for lower solid volume fraction samples.

3.2. Pore filling and pore coarsening

Pore filling and coarsening was observed in higher liquid volume fraction samples. During the initial stages of LPS, because of the low solubility ratio, liquid copper wets the solid particles and flows into capillary, leaving pores in original Cu sites [5]. Since the green compact has some initial porosity, about 30% [21], pores coalesce within the compact during the melt. Fig. 9 shows a photograph of 70vol%Co-Cu sample after 2.5 min sintering. Even the solid volume was high in this sample, the pores were well developed. These pores obtain a size that cannot be destabilized by the presence of the solid particles. These pores eventually become surrounded by particles that distort the liquid-vapor interface.

As the particles grow, the radius of the liquid meniscus between particles increases. As a result of this growth, a pressure difference draws liquid into the pore [23, 24], thus reducing the pore radius and increasing densification. Pore filling in the Co-Cu system was considerably more significant than that in Fe-Cu system. Fig. 10 shows a picture of pore after pore filling.

The mechanics of pore filling has been discussed by Park *et al*. As an assumption, the surrounding particles are closed-packed and of a uniform size with liquid menisci between them [24]. If the pore is spherical, filling will be uniform from all sides. In the case of an irregular pore, the region that has the smaller radius will fill first with the region of larger radius filling later.

Those assumptions were necessary for pore filling. However, observations with Fe-Cu and Co-Cu samples processed in microgravity showed particles were always in different sizes. The microstructure from short time sintering samples, such as 2.5 min samples, showed a irregular pore was trimmed during particle rearrangement stage by particle and pore rearrangement, which may not be the results from particle growth. Samples processed longer than 5 min showed that many pores were not filled but were partly broken into two parts of different sizes. The small size part could be filled because of the pressure changes once brokenup rather than the growth of particles surrounding the pore. In this paper, a new initiation mechanism will be introduced which will be used to explain the pore breakup and pore filling that was observed in microgravity liquid phase sintering.

Similar to particle growth, pore coarsening due to Ostwald ripening is also observed. For different solid

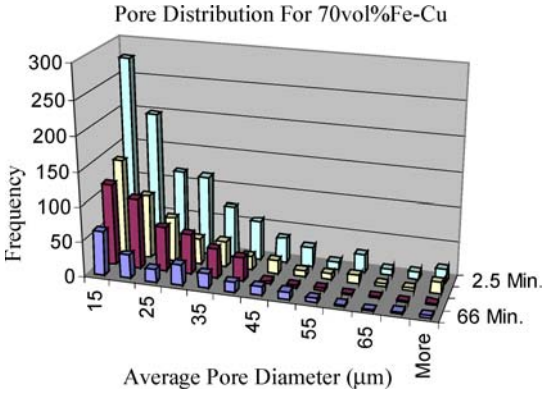

Figure 11 The pore size distribution of 70vol%Fe-Cu sample.

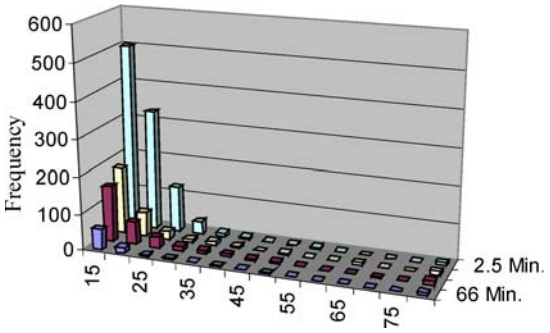

Figure 12 The pore size distribution of 70vol%Co-Cu sample.

volume fraction samples, as the sintering time increased, the total number of pores observed decreased and the size of pore increased. Figs 11 to 12 shows the pore distribution as a function of sintering time and liquid volume fraction. As the sintering time increased, the total number of pores decreased and the pore size became larger. As the liquid volume fraction increased, the total number of pores decreased quickly because volume diffusion of pore became more significant. The size of pore also became larger.

As the processing time increased, the chances for pore filling or breakup was much less. But the pore growth during prolonged heating would be more rely on the Ostwald ripening and the final number of pores would be fewer and fewer. For samples processed in microgravity, the pore size would become larger (of course some smaller one would disappear). A critical pore size could be reached when equilibrium is satisfied. From this point of view, together with the fact that, in most microgravity processed samples, the largest pores are always surrounded by particle without being filled, the observed pore filling after prolonged sintering might be the results of long sintering time. Because smaller pores continue to shrink due to the volume diffusion other than grain growth.

4. Discussion

Evidence of the pore metamorphosis from microgravity processed samples showed some snapshots of pore behaviors, which are otherwise obscured by gravity. In the last several decades, some studies on morphological stability of pores have been published using Rayleigh's instability theory and bubble's fluid dynamic property [25]. Later in Moon and Koo's study [10] on bubble formations during solid phase sintering, mass transport during sintering was considered combining with instability theory. The study of the low Reynolds number deformation and breakup of a gas bubble due to a non-uniform velocity field is a classical free-boundary problem which has been of interest in fluid mechanics for a long time. However, the bubble problem in liquid phase sintering samples is more difficult to model than the conventional bubble problem because of the existence of particles. Recently, pore-filling theory has been used to monitor the liquid phase sintering process with the focus of the particles growing effects on the shape of pore [26]. However, it ignored other pore metamorphosis effects during the process. There are many transport and kinetic effects contributing to the microstructure and pore distribution seen in microgravity and unit gravity processed LPS systems. These include the solubility between the phases, wetting of the liquid, grain boundary penetration, capillary forces, grain growth, and non-ideal viscous effects in a coupled solid/liquid molten phase. In addition to the above, process variables such as particle size, solid volume fraction, sintering temperature, time, atmosphere, and initial green densities have profound effects on resulting microstructures.

The microgravity processed samples showed us a full scene on the pore metamorphosis where pore showed bifurcated behaviors based on their system properties. To understand what happened during pore metamorphosis, let's first look at some key factors that affect the pore metamorphosis.

4.1. Solid volume fraction and surface diffusion

Moon and Koo [10] studied bubble formation in solid phase sintering and showed a surface diffusion controlled bubble shape accommodation. They derived an equation for the separation distance of pores in solid phase sintering. Based on Rayleigh's initial work and the measured pore sizes following break up to λ_m, they determined that the pore breakup by surface diffusion of vacancies resulted in $\lambda_m = 2.43$d, and pore breakup by volume diffusion resulted in $\lambda_m = 2.94$d, where d was the pore diameter following the breakup [10]. For a system with fluid phase, computer fluid dynamic simulations have proved that instability couldn't simulate bubble breakup well with extensional flow existence [27]. However, the surface diffusion and volume diffusion do exist in all LPS systems. It is obvious that the liquid bridge shown in Fig. 7 couldn't be the result of liquid flowing, but is the result of surface diffusion. For this 80vol%Fe-Cu sample, because of the liquid wetting and solving on Fe particles (Cu have higher solubility on Fe), and the strong capillary forces that hold the liquid Cu from flowing into the pore, no excess liquid can be further transferred or flow into the pore. This results in a skeleton structure and no fully breakup of the pores even after 330 min sintering. For 70vol%Fe-Cu sample, the excess of liquid makes it

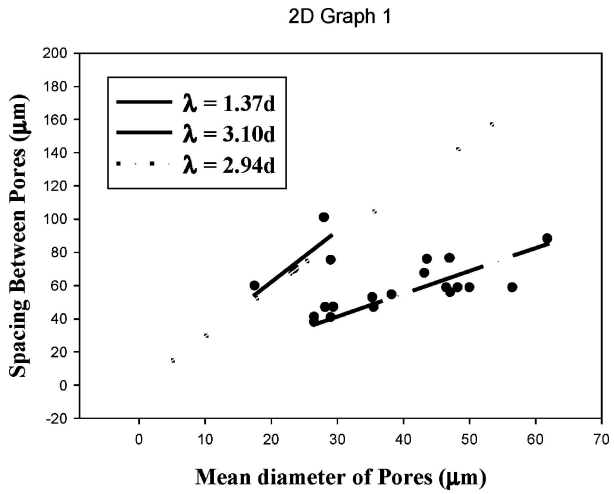

Figure 13 Center-to-center separation distance between spherical pores vs. diameter of pores following breakup at various processing times.

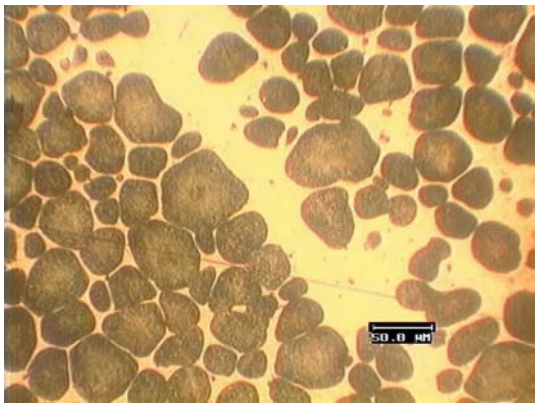

Figure 14 Agglomeration in microgravity processed Co-Cu sample, (1) closed packed particles, (2) Liquid copper pool, (3) Loosely packed particle zone.

possible for pore to further breakup. Because of the existence of particle agglomeration and relatively high solid volume fraction in this sample, solid diffusion does exist in 30vol%Fe-Cu samples. The governing equation for pore breakup due to the volume diffusion is described as [4, 10]:

$$\frac{\partial n}{\partial t} = B\nabla_s^2 K \quad \text{with} \quad B = \frac{D_s \gamma \nu \Omega^2}{kT}$$

where D_s = volume diffusion coefficient (isotropic), γ = surface tension, ν = number of diffusion atoms per unit surface area, Ω = Atomic volume, k = Boltzmann's constant, T = absolute temperature, $\nabla s^2 K$ = surface Laplacian of K and K is the mean curvature of the surface. Based on this equation, Moon *et al*. has derived that for volume diffusion controlled pore breakup, the separation distance is $\lambda_m = 2.94$d.

The pore separation distances for various pore diameters were measured before for Fe-Cu system and is shown in Fig. 13. Following Gupta's treatment [28], only those spherical pores that appear to be regularly aligned after ovulation were considered. The data were taken from 30vol%Fe-Cu samples processed in Space Shuttle. The data can be interpreted as two parts. The solid line showed the effects of volume diffusion because of the particle agglomeration and the high local solid-volume fraction in 30vol%Fe-Cu samples, which provide a near-solid phase sintering environment. The dashed line in that figure shows a bubble separation mainly caused by fluid properties inside the sample. A least square fit of the data gave a slope of 1.37d (Fig. 13). This part will be discussed in next section.

One would expect the liquid-solid vapor results for LPS to reside between the liquid-vapor and the solid vapor results. It is clear from Fig. 13 that this is not the case. The most likely reason for this deviation is the presence of small solid particles within the liquid phase that is in contact with the pore interface which caused local solid sintering which enhanced pore breakup by surface diffusion similar to what Moon and Koo has described. These particles significantly alter the capillary force action on the pore, and consequently the pressure distribution in the liquid surrounding the pore. For higher liquid volume fraction samples, solid sintering may also be enhanced by agglomeration of particles.

In ground processed samples, agglomeration and coalescence were mainly attributed to sedimentation by gravitational force, which led to pore evacuation and high grain growth rate. Even in microgravity where settling no longer exists, the agglomeration due to the weak interaction forces still exists [29]. Other process, such as liquid wetting particles, liquid penetration due to the surface tension and pore filling (liquid ejection), may also attribute to the agglomeration. Fig. 14 shows an agglomerated particle zone is seen adjacent to a liquid copper pool formed by liquid ejection in a Co-Cu sample. A previous study [29] of LPS in the Fe-Cu system under microgravity indicated similar behavior that was attributed to agglomeration of the Fe particles. Observations with different solid volume fraction samples showed a decrease in tendency on agglomeration as solid volume fraction increased. This appears to be reasonable because Cu has higher solubility in Co or Fe and a skeletal structure is easy to generate in higher solid volume fraction samples, which prohibited further agglomeration. Also, comparing to the agglomeration in Fe-Cu samples, the solid volume fraction for Co-Cu to generate skeletal structure is smaller than that for Fe-Cu samples. Combined with better wetting of Cu on Co, faster Co grain growth and consequence less grain number, it is reasonable to believe that pore breakup is easy to occur in Fe-Cu sample than that in Co-Cu sample with same solid volume fraction. The results from dihedral angle and contact per grain and coordination number also showed the indication of agglomeration in those samples.

The pore breakup due to the surface diffusion does not apply to the high liquid volume fraction samples. As the liquid volume fraction increases, the effects of volume diffusion (or Ostwald ripening effect) become dominant. The volume diffusion results in pore coarsening where small pores disappear and larger pores become larger. Therefore pore fillings in prolonged sintering samples may be the results of volume diffusion too.

4.2. Grain growth and initiation mechanism

Consider a pore that is surrounded by solid particles that bind together by capillary force driven agglomeration induced by the liquid phase. As the particles grow, the radii of the liquid meniscus between particles increase. As a result of this growth, a pressure difference draws liquid into the pore, thus reducing the pore radius and increasing densification [10]. It has been found that both Fe-Cu and Co-Cu showed pore filling in high liquid volume-fraction samples.

For the lower liquid volume-fraction samples, say 30%, non-uniform grain growth may lead to liquid flowing into the local meniscus and generate interparticle forces associated with this flow. This will result in pore breakup. In this way some larger pores which cannot be filled due to the large pore radius can eventually undergo breakup at some point, depending on their initial size. To verify the liquid impact effect, a CFD code on bubble formation in a liquid system was applied to the Fe-Cu system [30]. The governing equation is described as:

$$\frac{\partial \vec{u}}{\partial t} + \bar{u} \cdot \nabla \vec{u} = \frac{1}{\rho}\left(-\nabla P + \frac{\mu}{Re}\nabla^2 \vec{u} + \vec{F}_{\mathrm{st}} \right)$$

$$\text{with } \nabla \cdot \vec{u} = 0$$

$$\rho = \rho_1(1-f) + \rho_2 f$$

$$\mu = \mu_1(1-f) + \mu_2 f$$

$$\frac{\partial f}{\partial t} + \vec{u} \cdot \nabla f = 0$$

$$\vec{F}_{\mathrm{st}} = \sigma \cdot \kappa(x) \cdot \vec{n}\ (x_s)$$

where F_{st} is the force associated with surface tension.

The results are shown in Fig. 15 , which shows a cylindrical bubble that breaks into two small bubbles under a vertical flow impact to the pore. The separation distance shows a nearly 1.2 times of the pore diameter. The dash line in Fig. 13 shows a slope about 1.37. Given the influence of particle or the volume diffusion, it is reasonable to say that solid line is the result of the fluid mechanics that associated with grain growth.

The latest microstructure study showed that the microgravity liquid phase sintering does not produce a static system [14, 29]. Besides of particle rearrangement, agglomeration occurs during the sintering process. In the absence of gravitational force, several forces could contribute to the agglomeration of the solid particle in microgravity. These include the capillary force which generate liquid flow and particle movement to form agglomerates; Brownian motion, which is a weak force in unit gravity processing, is relative strong compare with stokes force in microgrvity and could be a major contributor to the agglomeration. These forces could generate a strong local convection flow which could break the pore in half.

4.3. Pore filling and coarsening

The pore filling mechanism presented by Kang *et al.* [31, 32] are still valid for the pore changes during solution-reprecipitation stage. However, since volume diffusion also dominate in solution-reprecipitation stage and solid sintering stage, some smaller size pore will be filled mostly because of volume diffusion rather than grain growth. On the other hand, the meniscus changes due the local grain growth may generate a convection flow due to the capillary force, which may change the local surface tension can cause larger pore break up.

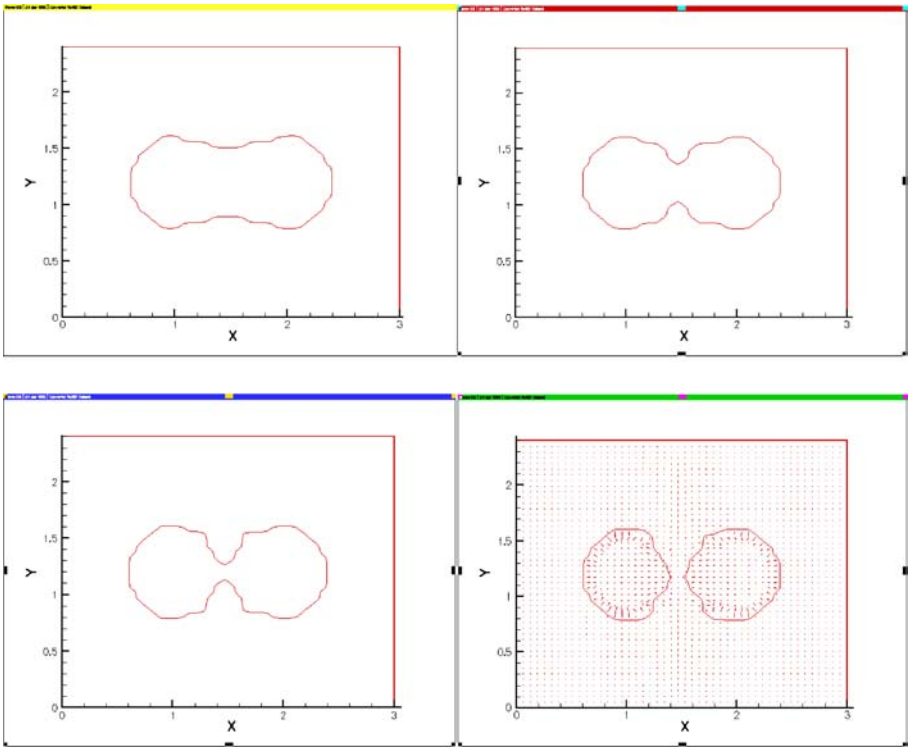

Figure 15 CFD simulations on a cylindrical bubble breaks up into two small bubbles under an initial perturbation in longitude direction.

The pore size will continue to grow based on volume diffusion at the expense of smaller pores. The equilibrium pore size is associated with process pressure and temperature. The Kelvin equation can be used to approximate the equilibrium pore size. The surface free energy change for a bubble with radius r is [33, 34]:

$$\Delta G_{\text{surface}} = 4\pi r^2 \gamma$$

where γ is the interfacial tension. The free energy change of maintain a bubble with radius R is given as:

$$\Delta G = -4\pi r^3 \frac{\Delta G_v}{3} \text{ and } \Delta G_v = \frac{kT \ln \alpha}{O} = \frac{RT}{\nu} \ln \frac{P}{P_0}$$

where O is the molecular volume of bulk phase, ν is the molar volume. The total free energy change required to maintain a bubble of radius r is:

$$\Delta \mathrm{G} = 4\pi r^2 \gamma - \frac{4\pi r^3}{3\nu} \mathrm{RT} \ln \frac{P}{P_0}$$

This equation shows a maximum in ΔG occurs at some intermediate value, R_C. Fig. 16 illustrates the variation of ΔG with r using Fe-Cu liquid phase sintering as an example. At the maximum, $d(\Delta G)/dr = 0$. If a Fe-Cu sample is processed in near vacuum condition, the calculation yields a critical radius of 1200 micron. The examination of sintered Fe-Cu aboard Mir Station showed the largest pore diameter of 2 mm after 330 min sintering, which is very close to the equilibrium pore size.

The samples processed in Argon environment (samples processed aboard Sounding Rockets and the Space Shuttle), the results would be a little different. However, the pore coarsening via volume diffusion mechanism is the same.

4.4. Densification

Densification is an important aspect of all LPS manufacturing operations. The elimination of pores and the production of a fully dense compact are the goal

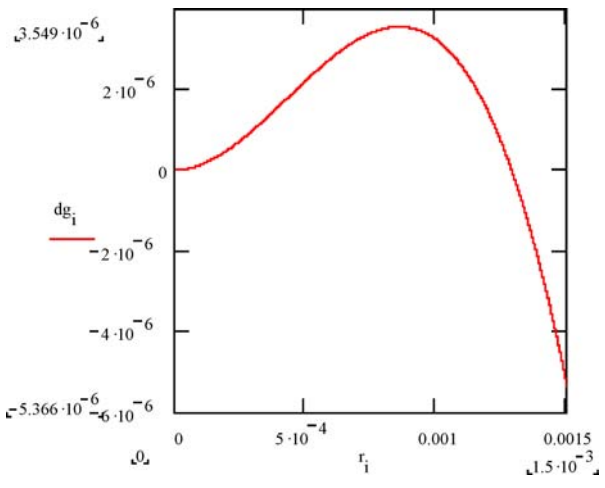

Figure 16 Change in free energy ΔG, with radius r of a spherical bubble.

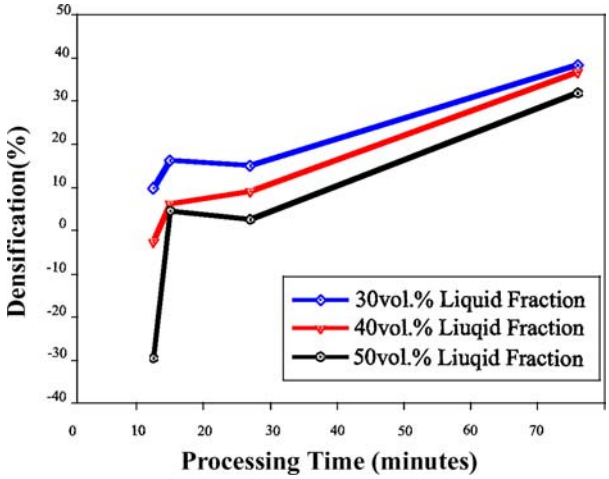

Figure 17 Densification of Co-Cu samples at different sintering time.

of all powder metallurgical processes with the exception of the production of porous materials. Because of the existence of pore in microgravity-processed sample, the liquid phase sintering theory for microgravity processing would be mainly associated with pore morphological changes. Lee *et al.* [26] has tried to describe the liquid phase sintering theory via pore filling theory using the ground-processed samples. The analysis of our microgravity processed samples showed that pore morphological changes are not limited on pore filling, but are the combination of pore filling, pore breakup and pore coarsening. Using the pore size distribution in Figs 11 and 12, the pore metamorphosis theory can be derived.

Here, the normalized volumetric shrinkage (densification) for the Co-Cu samples and for Fe-Cu samples as a function of time is presented in Figs 17 and 8. It clearly shows that the pore filling via initiation mechanism is the major cause of densification. The initial densification drop is due to the low solubility ratio that generates swelling effect during the rearrangement stage of liquid phase sintering. Then the densification increased as more pores are filled. Fe-Cu samples processed in Mir Station showed that highest liquid volume fraction samples has lowest densification because pore coalescence and coarsening is more dominant based on bifurcation theory, which is similar to what have found in Fe-Cu samples processed aboard Sounding Rockets and the Space Shuttle.

5. Conclusion

Examples of pore morphological changes in microgravity-processed samples are presented in this paper. Pore showed bifurcated behaviors based on their liquid volume fraction. For low liquid-volume fraction samples, the initiation mechanism is valid for pore breakup via volume diffusion mechanism. Grain growth during liquid phase sintering would generate local pore filling. Together with the instability and weak force effects, the pore will break up due to the initiation mechanism. The large pore breakup via irregular dumbbell shape must be the results of initiation mechanism. Ostwald ripening of pore occurred throughout the entire process, though a equilibrium pore size

exists based on Kelvin theory. With the help of particle growth, which provided more excess liquid, pore continued to metamorphosis. Pore breakup and pore filling in Co-Cu and Fe-Cu sample lead to high densification. Combined with pore coarsening, the morphological changes define the liquid phase sintering theory in microgravity.

Acknowlegement

This work was supported by NASA under a joint agreement with the Consortium for Materials Development in Space at the University of Alabama in Huntsville. Numerous individuals across two continents have contributed their knowledge, cooperation and support to this project.

References

1. W. J. HUPPMANN and G. PETZOW, in Sintering Processes, edited by G. C. Kuczynski (Plenum Press, New York, NY, 1980) p. 189.
2. Y. HE, S. YE, A. K. KURUVILLA, J. E. SMITH, JR., A. IVANOV, U. BRATUKIN and G. PUTIN in 4th International Symposium on Self-propagating High-temperature Synthesis (Telodo, Spain, October 6-10, 1997).
3. S. KIM, J. NOH and K. CHURN, *J. Mater. Sci*. **8** (1989) 1320.
4. R. M. GERMAN, Liquid Phase Sintering (New York, Plenum Press, 1985).
5. C. M. KIPPHUT, A. BOSE, S. FAROOQ and R. M. GERMAN, *Metallurgical Transactions A*. **19A** (1988) 1905.
6. T. H. COURTNEY, *Scripta Met.* **35**(5) (1996) 567.
7. D. R. LIDE, Editor-in-Chief, "CRC Handbook of Chemistry and Physics," in 72nd Edition, CRC Press (Boca Raton, Ann Arbor, Boston, 1991–1992).
8. D. F. HEANEY and R. M. GERMAN, Advances in Powder Metallurgy and Particulate Materials (Metal Powder Industries Federation, Princeton, NJ, 1994) vol. 3, p. 303.
9. Y. HE, A. K. KURUVILLA and J. E. SMITH JR., in 10th International Symposium on Experimental Methods for Microgravity Materials Science, TMS publication, compiled and edited by Dr. Robert A. Schiffman (1998).
10. D. M. MOON and R. C. KOO, *Metall. Trans. A* **2** (1971) 2115.
11. Z. XUE, J. G. VANDEGRIFT and A. K. KURUVILLA, *Mater. Trans., JIM* **37** (1996) 1084.
12. S. NOOJIN, J. G. VANDEGRIFT, K. HARTMAN and J. E. SMITH JR., "Study of the Gravitational Effects on the Rearrangement Stage of Liquid Phase Sintered Binary Metallic Alloys" (ASME Heat Transfer Div. Pub., 1993) Vol. HTD 259, p. 127.
13. E. ATCHLEY, T. HAMILTON, A. HEDAYAT, J. G. VANDEGRIFT and J. E. SMITH JR., "Overview and Preliminary Modeling and Ground-Based Results for the ECLiPSE," 8th International Symposium on Experimental Methods for Microgravity Materials Science, TMS publication, (Available in CD-ROM format only), edited by Dr. Robert A. Schiffman (1996) p. 87.
14. Y. HE, S. YE, J. NASER, J. CHIANG and J. E. SMITH, JR., *J. Materials Sci*. **35**(23) (2000) 5973.
15. S. NOOJIN, "Master Thesis" (University of Alabama in Huntsville, 1989).
16. J. G. VANDEGRIFT, S. L. NOOJIN and J. E. SMITH JR., *J. of Spacecraft and Rockets* **34**(1) (1997) 104.
17. R. M., GERMAN, "Powder Metallurgy Science" (Metal Powder Industries Federation, Princeton, New Jersey, 1984).
18. J. G. VANDEGRIFT, "Master Thesis" (University of Alabama in Huntsville, 1996).
19. Z. XUE, S. NOOJIN, J. G. VANDEGRIFT and A. K. KURUVILLA, Experimental methods for Microgravity materials Science, edited by Robert Schiffman (TMS Publications, 1996) in press.
20. Z. XUE, S. NOOJIN, J. G. VANDEGRIFT and A. K. KURUVILLA, *High Temperatures-High Pressures* **29** (1997) 349.
21. Z. XUE, "Master Thesis" (University of Alabama in Huntsville, 1995).
22. S. YE, A. K. KURUVILLA, Y. HE and J. E. SMITH, JR., Optizone Liquid Phase Sintering Experiment (OLiPSE-01) (NASA 2 Final Research Report), Phase 1 Research Program Quarterly Research Report, Sixth Quarterly Report, pp1-3 - 1-14, National Aeronautics and Space Administration, Lyndon B. Johnson Space Center, Houston, TX, August 1998.
23. H. PARK, S. CHO and D. YOON, *Metallurgical Transactions A.* **15A** (1984) 1075.
24. H. PARK, O. KWON and D. YOON, *Metallurgical Transactions A* **17A** (1986) 1915.
25. L. RAYLEIGH, *Proc. London Math. Soc*. **10** (1878) 4.
26. S. LEE and S. L. KANG, *Acta Mater*. **9** (1998) 3191.
27. H. A. STONE and L. G. LEAL, *J. Fluid Mech*. **198** (1989) 399.
28. T. K. GUPTA, *J. Am. Ceram. Soc*. **61** (1978) 191.
29. J. NASER, A. K. KURUVILLA and J. E. SMITH, JR *Journal of Materials Science* **33** (1998) 5573.
30. F. QI and C. P. CHEN, "Two-phase flow simulation using a combined volume-of-fluid/level-set method", Alabama Space Consortium, to be published, Jan. 1999.
31. C. H. KANG and D. N. YOON, *Metallurgical Transactions A*. **12A** 65 Jan. 1981.
32. KANG, S. S. and YOON, D. N., *Metallurgical Transactions A*. **13A** 1405 Aug. 1982.
33. D. J. WEDLOCK, "Controlled particle, Droplet and Bubble Formation" (Butterworth-Heinemann Ltd, 1994).
34. R. J. STOKES and D. F. EVANS, "Fundamentals of Interfacial Engineering" (Wiley-VCH, Inc., 1997).

Received 20 October 2003
and accepted 7 March 2005